

Effect of Axial Groove on Steady State and Stability Characteristics of Finite Two-Lobe Hybrid Journal Bearing

Lintu Roy*

Department of Mechanical Engineering, National Institute of Technology, Silchar-788010, India

Abstract

The study of the steady state and stability characteristics including whirl instability of finite two-lobe hybrid journal bearing with an axial groove, located at the top from which oil is supplied at a constant pressure is obtained theoretically. The two lobes of 1600 arc each are separated by two axial oil groove of 20° circumferential extensions in the horizontal direction. A two-dimensional finite difference solution was used to predict the performance of finite length externally pressurized two-lobe hydrodynamic hybrid journal bearings. The Reynolds equation is solved numerically using finite difference method satisfying the appropriate boundary conditions to obtain the effect of speed parameter on bearing performance. The stability characteristics were found out using first-order perturbation method. With the change of speed Stiffness and damping coefficients behaviour was determined at various eccentricity ratios. The bearing load-carrying capacity, stiffness, lubricant flow rate, attitude angle and frictional torque due to bearing rotation increase with increase in eccentricity ratio and speed. A comparison is also made with plain cylindrical axial grooved journal bearing. It is found that externally pressurized two-lobe hybrid bearing is more superior to plain cylindrical axial-grooved oil journal bearing in terms of load capacity, improved end flow, friction losses and stability. The bearing is generally stable at high values of the eccentricity ratio and speed parameter.

Keywords: Axial groove; Two-lobe hydrodynamic journal bearing; Steady state and stability characteristics

Introduction

The quantity of oil flow in a journal bearing plays an important role in maintaining an uninterrupted oil film and removing most of the frictional heat to cool the bearing. The oil flow rate depends on several factors, such as the viscosity of the lubricant, the geometry (length, diameter and radial clearance) of the bearing, operating eccentricity, the inlet oil pressure and the arrangement of feeding sources. The pressure developed in the film due to journal motion also contributes to the flow. One of the simplest ways of feeding oil is a single hole through the bearing which is usually a stationary member at the unloaded region. This ensures higher pressure development in the larger land area in the clearance space. The external radial load on such a bearing should be unidirectional and constant in magnitude. However, the direction of applied load may vary only within relatively narrow limits so that the oil hole remains always in the unloaded region.

In an internal combustion engine bearing both the magnitude and direction of load changes. In such a situation the location of an oil hole in the unloaded region is not possible. This is overcome by feeding oil through a circumferential groove at the mid plane. This will naturally reduce the load capacity because of reduced land area. This bearing can cope up easily with the condition when both the direction and magnitude of load vary. However an elaborate arrangement of the feeding system is to be designed. Oil is also fed by providing an axial groove in the unloaded region. Ordinary circular bearings were not found to be very stable at such high speeds. This gave rise to some new designs of bearings by changing their geometries, such as multilobe bearings and pressure dam bearings, which were found to possess better stability. Hydrodynamic bearings operating at high speeds are often confronted with problems of instability, known as whirl and whip. Instability may ruin not only the bearings but the machine itself. Satisfactory dynamic characteristics are an essential requirement of a good bearing design and bearings of non-circular cross-section hold good promise for applications where bearing stiffness and stability are major considerations. Non-circular bearing geometry enhances shaft

stability and under proper conditions, this will also reduce power losses and increase oil flow (as compared to circular bearings), thus reducing bearing temperatures. Among the non-circular sleeve bearings, elliptical and three lobe bearings are most commonly used. Extensive literature is available on circular bearings but the data available for the design of non-circular bearings is comparatively scarce. The steady state load capacity and power losses for elliptical bearings have been calculated by Pinkus [1,2] using finite difference method. The computation procedure for the stiffness of externally pressurized bearings relies on an analytical description given in some previous papers [3,4]. Lund [5] developed the stability criterion for a multilobe bearing based on linearization of Reynolds equation by small perturbation theory. Falkenhagen and Gunter [4] investigated the stability of a vertical rotor and evaluated the hydrodynamic forces by finite difference analysis and an approximate method. In an internal combustion engine both magnitude and direction of load changes. A novel method to cope up with this situation is the use of submerged oil bearing proposed by Floberg [6]. The friction characteristics of externally pressurised bearings are investigated in [7] over a complete range of operating bearing conditions. Geometrical characterizations of externally pressurized journal bearing have been defined [8]. Falkenhagen et al. [9] investigated the stability characteristics and transient motion of a finite width three-lobe bearing for a wide range of ellipticity ratio and offset factor. Lund and Thomson [10] gave some design data which included both static and dynamic characteristics for laminar as well as turbulent flow regimes. A comparison of non-dimensional values of steady state and dynamic characteristics for two-lobe bearing has been made with

*Corresponding author: Lintu Roy, National Institute of Technology, Silchar-788010, India, Tel: +919435300307; E-mail: lintu2003@gmail.com

Received July 25, 2014; Accepted August 13, 2014; Published August 20, 2014

Citation: Roy L (2014) Effect of Axial Groove on Steady State and Stability Characteristics of Finite Two-Lobe Hybrid Journal Bearing. J Appl Mech Eng 4: 146. doi:10.4172/2168-9873.1000146

Copyright: © 2014 Roy L. This is an open-access article distributed under the terms of the Creative Commons Attribution License, which permits unrestricted use, distribution, and reproduction in any medium, provided the original author and source are credited.

The non-dimensional steady state load components are given by

$$\bar{W}_X = \frac{4W_{Xs}}{LDp_s} = \int_{\theta_s}^{\theta_e} \int_0^1 \bar{p}_0 \cos \theta d\theta d\bar{z} \quad (4a)$$

$$\bar{W}_Z = \frac{4W_{Zs}}{LDp_s} = \int_{\theta_s}^{\theta_e} \int_0^1 \bar{p}_0 \sin \theta d\theta d\bar{z} \quad (4b)$$

The two-lobe bearings are suitable for a vertical load support, for calculating the vertical load an eccentricity ratio and attitude angle picked at random which results in magnitude of forces generated due to pressure wedge in the bearing can be calculated. The horizontal force (\bar{W}_Z) in the pressure wedge must be zero. If it is not this case a different value of attitude angle is chosen, where the sum of all the forces in the horizontal direction is again calculated. This will eventually locate the shaft at correct attitude angle and where the force in the horizontal direction is zero. Then for this equilibrium position, the vertical force (\bar{W}_X) gives the load carrying capacity \bar{W}_0

The Sommerfeld number can be given as $S = \frac{\Lambda}{3\pi\bar{W}_0}$

The end flow in each lobe in the dimensionless form can be written as

$$\bar{Q} = \frac{4Q\eta L}{C^3 D p_s} = -\frac{1}{3} \int_0^{2\pi} \bar{h}_0^3 \frac{d\bar{p}_0}{d\bar{z}} \Big|_{\bar{z}=1} d\theta \quad (5)$$

The friction variable is given by $\bar{\mu} = (R/C)\mu = \frac{\bar{F}}{\bar{W}_0}$ where

$$\bar{F} = \left(\frac{F}{2LCp_s} \right) = \iint 2 \left(\frac{h_0}{4} \frac{dp_0}{d\theta} + \frac{\Lambda}{12} \frac{1}{h_0} \right) d\theta dz \quad (6)$$

Dynamic characteristics

The Reynolds equation under dynamic condition is the equation (1). The pressure and film thickness can be expressed for small amplitude of vibration as:

$$\bar{p} = \bar{p}_0 + \varepsilon_1 e^{i\tau} \bar{p}_1 + \varepsilon_0 \phi_1 e^{i\tau} \bar{p}_2 \quad (7)$$

$$\bar{h} = \bar{h}_0 + \varepsilon_1 e^{i\tau} \cos \theta + \varepsilon_0 \phi_1 e^{i\tau} \sin \theta \quad (8)$$

\bar{h}_0 = the steady state dimensionless film thickness.

$$\varepsilon = \varepsilon_0 + \varepsilon_1 e^{i\tau} \quad (9)$$

And $|\varepsilon_1| \ll \varepsilon_0$ and $|\phi_1| \ll 1$

Substitution of equations (7) and (8) into the equation (1) and retaining the first linear terms, gives the three differential equations in \bar{p}_0, \bar{p}_1 and \bar{p}_2 . The equations for \bar{p}_1 and \bar{p}_2 are solved satisfying the modified boundary conditions of equation (3) and known values of \bar{p}_0 .

Dynamic loads due to \bar{p}_1 and \bar{p}_2 are given by

$$\bar{W}_{X1} = \int_{\theta_s}^{\theta_e} \int_0^1 \bar{p}_1 \cos \theta d\theta d\bar{z} \quad \bar{W}_{Z1} = \int_{\theta_s}^{\theta_e} \int_0^1 \bar{p}_1 \sin \theta d\theta d\bar{z} \quad \text{and}$$

$$\bar{W}_{X2} = \int_{\theta_s}^{\theta_e} \int_0^1 \bar{p}_2 \cos \theta d\theta d\bar{z} \quad \bar{W}_{Z2} = \int_{\theta_s}^{\theta_e} \int_0^1 \bar{p}_2 \sin \theta d\theta d\bar{z}$$

Dynamic forces of each lobe are added and total horizontal and vertical components are determined.

Stiffness and damping coefficients

It is found that the fluid film, which supports the bearing, is equivalent to a spring mass damping system. Since the journal executes small harmonic oscillations about its steady state position; the dynamic load carrying capacity can be expressed as a spring and a viscous damping force. The stiffness and damping coefficients are given by

$$\bar{K}_{XX} = -\text{Re}(\bar{W}_{X1}); \quad \bar{K}_{ZX} = -\text{Re}(W_{Z1}); \quad \bar{K}_{XZ} = -\text{Re}(\bar{W}_{X2});$$

$$\bar{K}_{ZZ} = -\text{Re}(\bar{W}_{Z2})$$

$$\bar{C}_{XX} = -\text{Im}(\bar{W}_{X1}); \quad \bar{C}_{ZX} = -\text{Im}(\bar{W}_{Z1}); \quad \bar{C}_{XZ} = -\text{Im}(\bar{W}_{X2});$$

$$\bar{C}_{ZZ} = -\text{Im}(\bar{W}_{Z2})$$

Mass parameter and whirl ratio

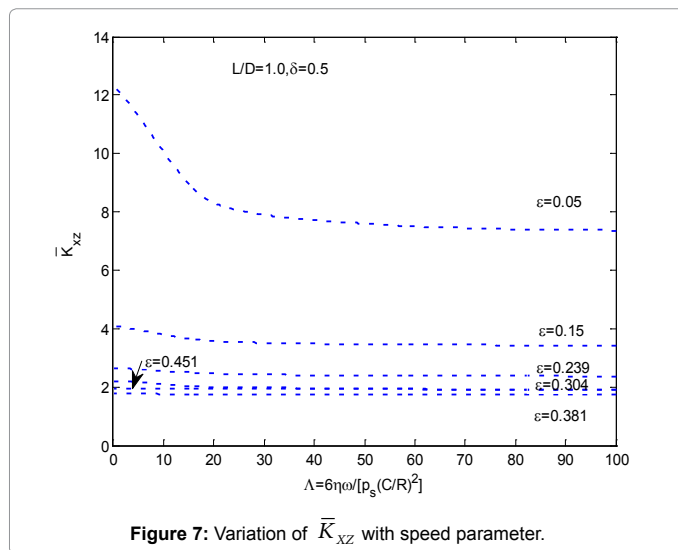
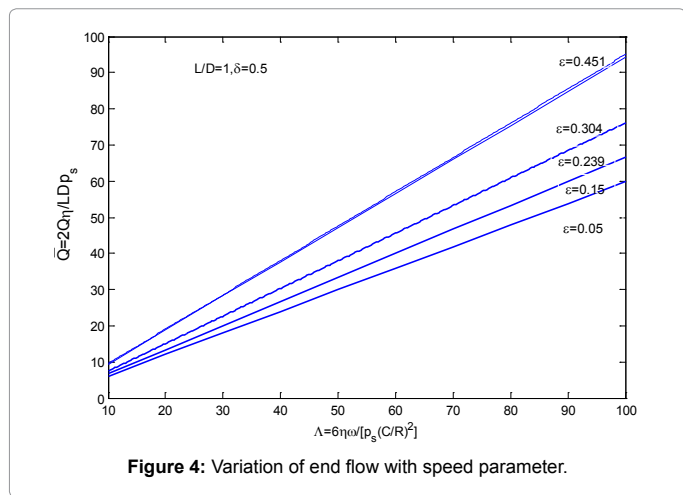
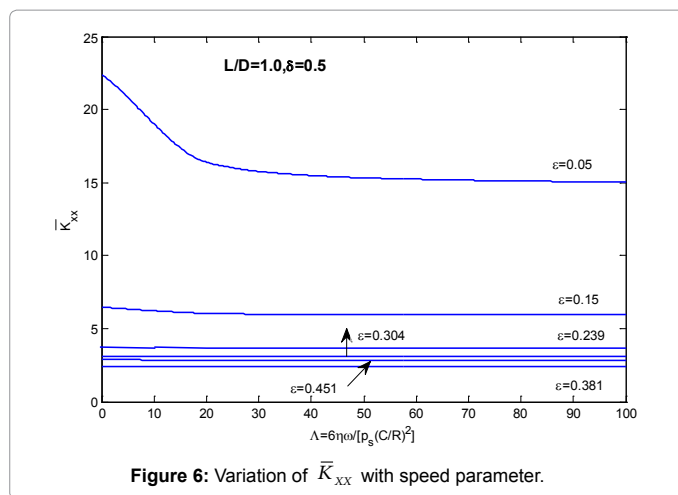
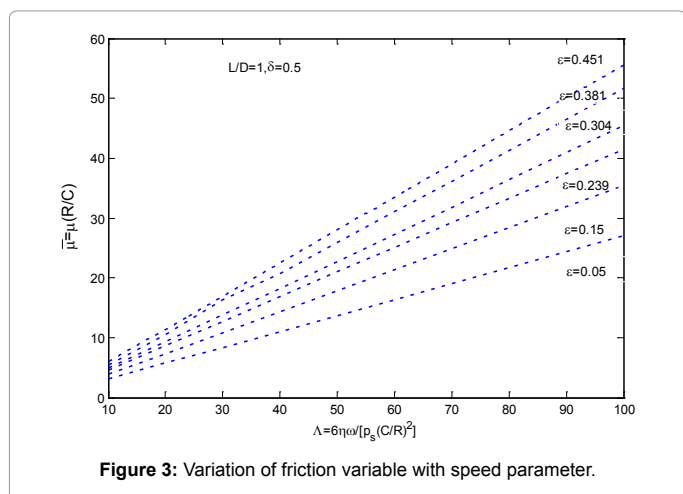
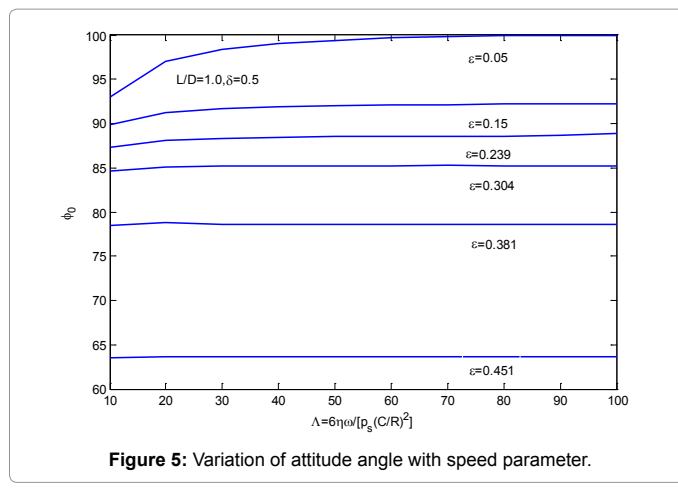
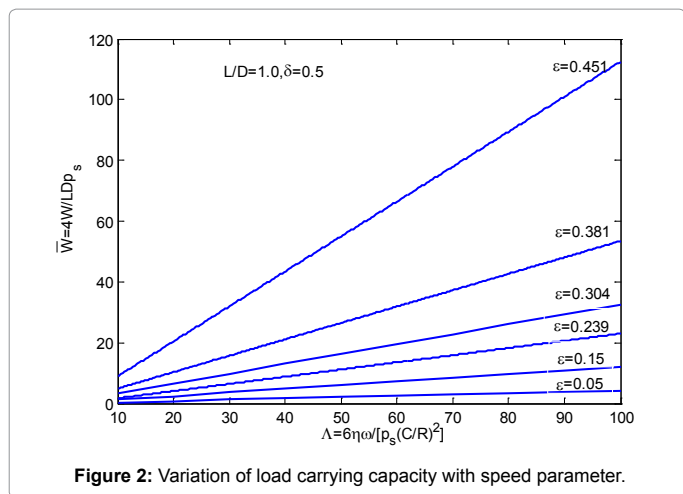
The mass parameter (\bar{M}) and whirl ratio (λ) according to [19] are related as

$$\lambda^2 \bar{M} = \frac{\bar{K}_{XX} \bar{C}_{ZZ} + \bar{K}_{ZZ} \bar{C}_{XX} - (\bar{K}_{XZ} \bar{C}_{ZX} + \bar{K}_{ZX} \bar{C}_{XZ})}{\bar{C}_{XX} + \bar{C}_{ZZ}} = k_0$$

$$\text{So, } \lambda^2 = \frac{(\bar{K}_{XX} - k_0)(\bar{K}_{ZZ} - k_0) - \bar{K}_{XZ} \bar{K}_{ZX}}{\bar{C}_{XX} \bar{C}_{ZZ} - \bar{C}_{XZ} \bar{C}_{ZX}} \quad \text{and } \bar{M} = \frac{k_0}{\lambda^2}$$

Results and Discussion

A computer program was developed, based on the present theory, to analyze the performance of a finite two-lobe hydrodynamic journal bearing with an axial groove. Before going to the present analysis the values of Sommerfeld number and stiffness and damping co-efficient obtained from the computer simulation of the ordinary two lobe bearing is compared with [10] and the obtained values are found to be matching. When the bearing operates at a small speed, the hydrodynamic effect is not predominant. The hydrodynamic pressure developed due to hydrodynamic action is insufficient to balance the applied load when fed from top. Thus it is difficult to run the bearing at low speeds. Therefore, there is a speed below which the bearing cannot be operated. In this present analysis, it has been found that the limiting value of non-dimensional speed parameter is $\Lambda = 6.5$. To be on the safe side, we have considered the speed parameter Λ is above 10. The variation of load carrying capacity, friction variable, end flow, attitude angle, stiffness co-efficient, mass parameter and whirl ratio for a bearing having groove length = $\frac{1}{4}$ of the total length of the bearing and 10° groove angle for 20° lobe angle is shown in Figures 2-17. Load capacity and friction variable increases with an increase in eccentricity ratio and speed. The load capacity increases with bearing number, which is a function of journal speed (Figure 2). This increase is sharp at higher eccentricity ratio. The rise in friction is particularly high at higher eccentricity ratios, as shown in Figure 3. The end flow increases with eccentricity and speed parameter (Figure 4). The attitude angle decreases with the increases in eccentricity ratio but it increases with the increase in speed parameter (Figure 5). A comparison has been done with plain cylindrical axial grooved oil journal bearing having groove geometry 18° and groove length $\frac{1}{2}$ and $\frac{1}{4}$ of the total bearing length (Table 1). It is observed that in comparison to the plain axial grooved bearing two lobe hydrodynamic journal bearing having improved performance in terms of load carrying capacity, end flow, friction characteristics and stability. The stability also improves for smaller groove angle and groove length. From the comparison with



ordinary plain two lobe journal bearing having $L/D=1.0, \delta=0.5$, $\Lambda = 10.0$, lobe angle $=20^\circ$ with present configuration of bearing with feeding groove angle $=18^\circ$ and groove length $\frac{1}{2}$ of the total bearing length, it is found that at higher bearing number the load capacity, mass parameter value tends to increase, hence an increase in critical mass parameter value (Tables 2 and 3). Direct stiffness co-efficient \bar{K}_{xx} is found to be

decreased with speed at lower eccentricity but at high eccentricity ratio the changes in stiffness magnitude less with speed (Figure 6). A similar pattern is found in case of \bar{K}_{zz} (Figure 9). The cross coupling stiffness \bar{K}_{zx} and \bar{K}_{xz} is found to increase in magnitude with eccentricity but the change is very little with the change of speed (Figures 7 and

ϵ	Groove length	\bar{W}	ϕ_0	\bar{Q}	$\bar{\mu}$	\bar{M}	λ
0.2	1/2	1.6069 (0.1145)	87.14 00 (83.0441)	7.2384 (0.6979)	4.1807 (49.0074)	3.2546 (2.9987)	0.4642 (0.5326)
	1/4	1.6551 (0.1865)	88.4100 (81.8925)	7.2001 (1.2346)	4.3296 (30.1540)	5.9365 (2.9270)	0.4660 (0.5543)
0.4	1/2	6.2487 (0.6831)	75.7600 (68.7400)	9.5725 (2.9266)	5.4969 (8.8515)	10.7621 (6.8051)	0.2804 (0.5740)
	1/4	6.2937 (0.7897)	75.9000 (67.6610)	9.5807 (2.4645)	5.6831 (7.6900)	10.9166 (6.5390)	0.2778 (0.5826)
0.451	1/2	11.6817 (0.81414)	63.3500 (65.4927)	9.4575 (1.8555)	5.9374 (7.6416)	16.7095 (10.154)	0.5550 (0.5737)
	1/4	11.7020 (0.93633)	63.5100 (64.5818)	9.4699 (1.5448)	6.1549 (6.6804)	18.2425 (8.6813)	0.5570 (0.5819)

Table 1: Comparison of results with plain cylindrical groove angle bearing having L/D=1.0, $\delta=0.5$, $\Lambda=10.0$, groove angle=18° and groove length=1/2 and 1/4 of total length of the bearing.

For the above table the numbers in the bracket's indicate the data obtained for axial grooved plain cylindrical journal bearing

ϵ	\bar{W}	ϕ_0	\bar{Q}	$\bar{\mu}$	\bar{M}	λ
0.2	1.6069 (1.7078)	87.14 00 (90.35)	7.2384 (7.1704)	4.1807 (3.4042)	3.2546 (6.2912)	0.4642 (0.4526)
0.4	6.2487 (6.3348)	75.7600 (76.0)	9.5725 (9.586)	5.4969 (4.8363)	10.7621 (11.1789)	0.2804 (0.2742)
0.451	11.6817 (11.7221)	63.3500(63.65)	9.4575 (9.4819)	5.9374 (5.0725)	16.7095 (21.4991)	0.5550 (0.2743)

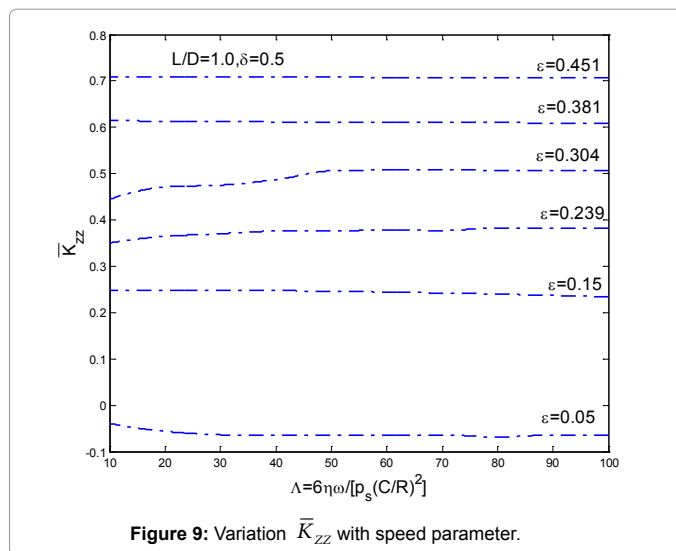
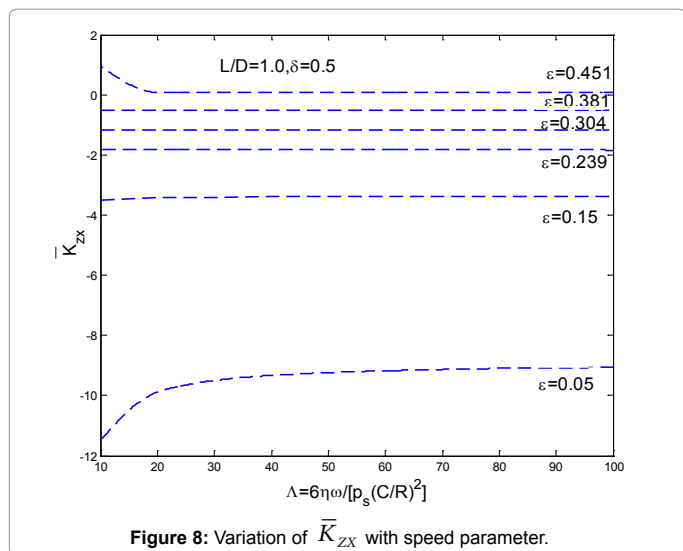
Table 2: Comparison of results with conventional two lobe bearing having $\delta=0.5$, L/D=1.0, $\Lambda=10.0$, lobe angle=20°.

For this table the numbers in the bracket's indicate the data for conventional two lobe bearing with feeding groove angle=18°

ϵ	\bar{W}	ϕ_0	\bar{Q}	$\bar{\mu}$	\bar{M}	λ
0.2	17.0204 (17.0887)	90.06 (90.33)	71.756 (71.7058)	4.1807 (38.5205)	4.2098 (6.2876)	0.4642 (0.4526)
0.4	63.3480 (63.348)	75.9965 (63.348)	95.8578 (95.8597)	5.4969 (52.8413)	12.6402 (11.1789)	0.2804 (0.2742)
0.451	117.275 (63.635)	63.6260 (63.635)	94.8004 (94.8074)	5.9374 (55.1996)	22.085 (21.7493)	0.47665 (0.2741)

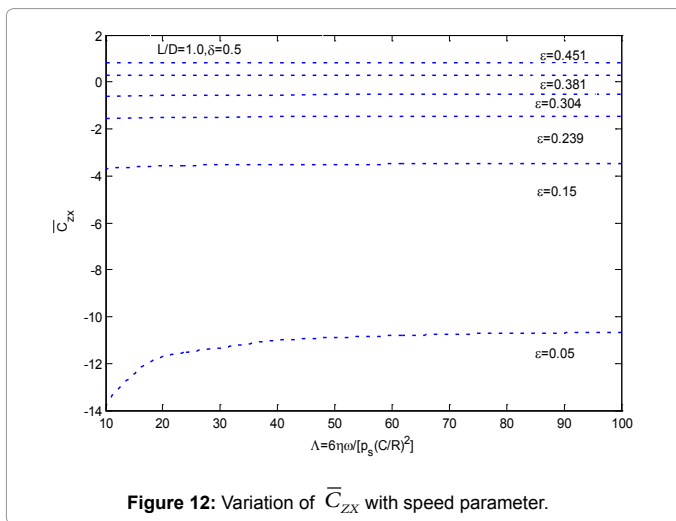
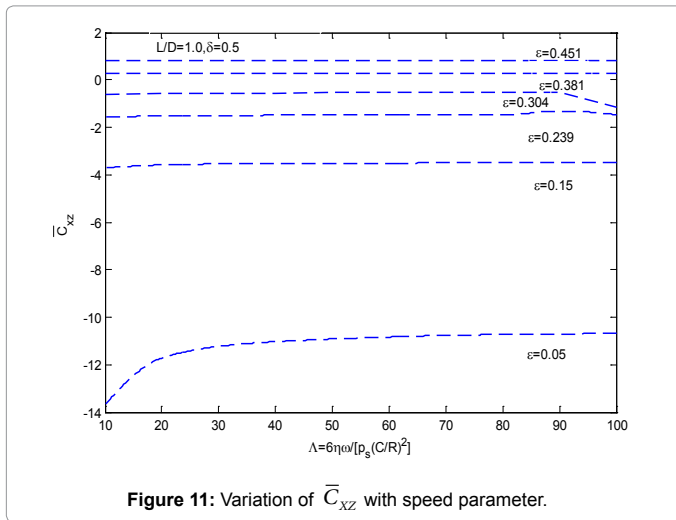
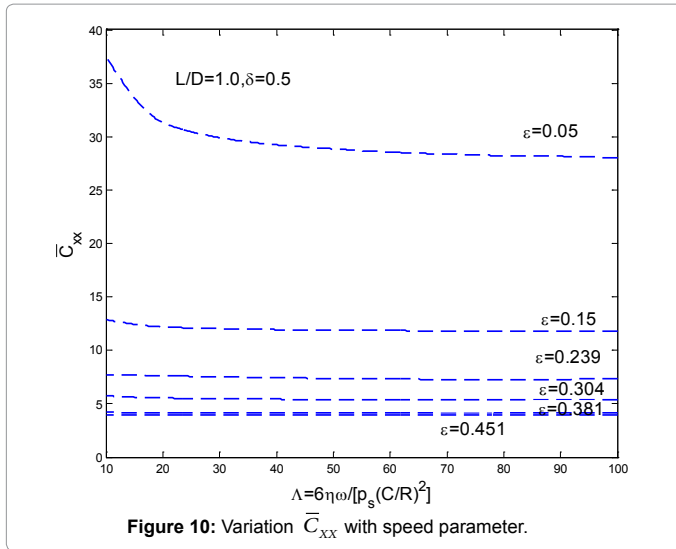
Table 3: Comparison of results with conventional two lobe bearing having $\delta=0.5$, L/D=1.0, $\Lambda=100.0$, lobe angle=20°

For this table the numbers in the bracket's indicate the data for conventional two lobe bearing with feeding groove angle=18°



8). Direct stiffness is not dependant on the speed generally, the cross stiffness affects the stability of the rotor and therefore its increase with speed generally indicates reduced stability of the rotor supported by the bearing [15]. Direct damping co-efficient \bar{C}_{xx} and \bar{C}_{zz} decreases at a low value of eccentricity ratio but at higher eccentricity ratio the change is very little with speed increase (Figures 10 and 13). Both the cross damping coefficient \bar{C}_{xz} and \bar{C}_{zx} increases gradually with the increase of speed (Figures 11 and 12). Direct damping is helpful in stabilizing the rotor supported by the bearing [15]. The mass parameter

\bar{M} and whirl ratio λ are used as a measure of stability. These are plotted in Figures 14 and 15. The upper portion of the curve is unstable and the lower portion of the curve is stable. The stability is found to increase with the increase of speed and eccentricity. It is observed that load capacity and stability also improves when smaller groove dimensions (Table 1) (i.e. smaller groove length and smaller groove angles) are used at higher speeds. As the mass parameter of the bearing increases and whirl ratio decreases as shown in Figures 14 and 15. This signifies that the bearing is more stable as the load carrying capacity increases

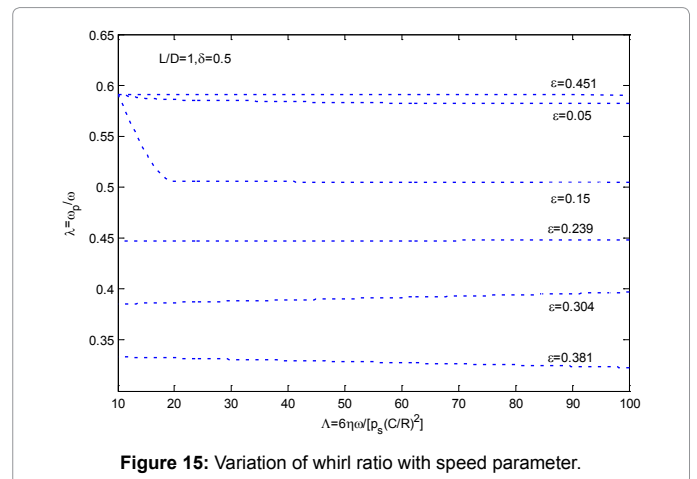
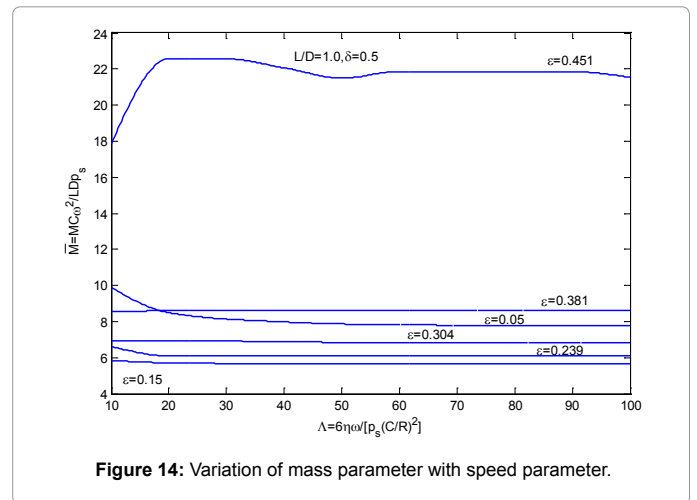
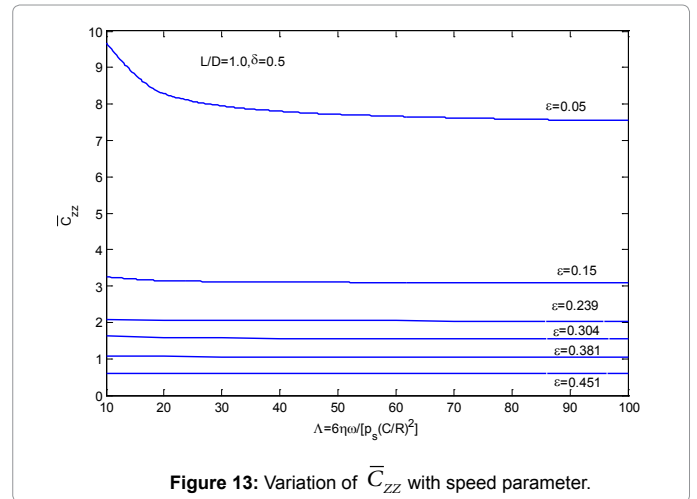


with eccentricity ratio. The mass parameter and whirl ratio variation with speed at a constant eccentricity ratio is shown in Figures 16 and 17. The mass parameter and whirl ratio decreases when groove length

changes from $\frac{1}{2}$ to $\frac{1}{2}$ Tables 1-3.

Conclusions

1. The bearing load capacity, the lubricant flow rate increases with increases in eccentricity ratio and speed parameter. This is due to the increase in journal speed.
2. The frictional torque due to journal rotation increases with



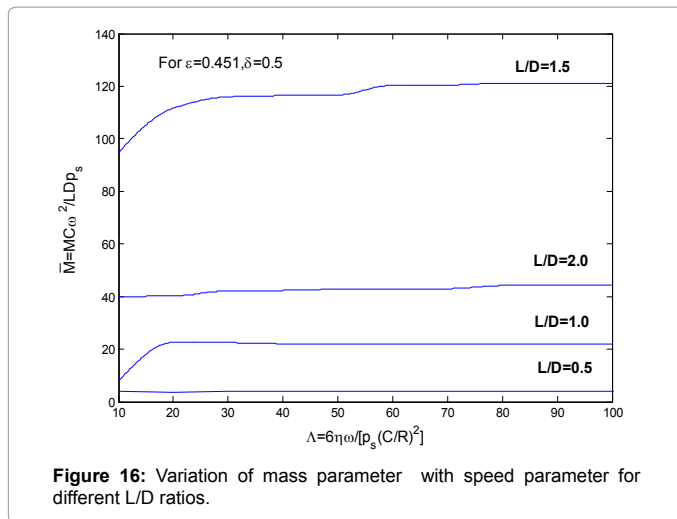


Figure 16: Variation of mass parameter with speed parameter for different L/D ratios.

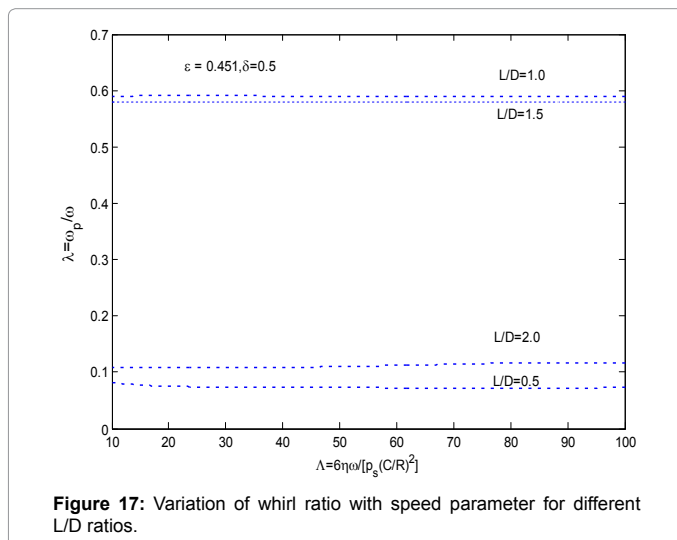


Figure 17: Variation of whirl ratio with speed parameter for different L/D ratios.

increases in the eccentricity ratio and speed of rotation.

3. At lower value of eccentricity ratio when the speed of the bearing increases the critical mass parameter remains almost the same and at higher value of eccentricity ratio it increases with speed and the whirl ratio decreases. At higher value of eccentricity ratio when the speed of the bearing increases the bearing becomes more stable.

At a lower value of eccentricity ratio both direct stiffness (\bar{K}_{xx} and \bar{K}_{zz}) and damping (\bar{C}_{xx} and \bar{C}_{zz}) co-efficient found to be decrease while at higher eccentricity ratio it remains more or less same as the speed increases.

At a higher value of eccentricity ratio the cross stiffness (\bar{K}_{xz} , \bar{K}_{zx}) and cross damping coefficients (\bar{C}_{xz} , \bar{C}_{zx}) is found to be increases as the speed increases.

4. The stiffness and damping coefficient magnitude is higher for the bearing fed from a smaller groove angle.

5. A bearing having smaller groove angle gives higher load capacity. This is due to high pressure in the land region.

6. The attitude angle increases with increases in the speed

parameter, and it is generally stable for higher values of the eccentricity ratio and speed parameter.

The data from the analysis these are presented in dimensionless form may be used in the design of such bearings.

References

1. Pinkus O (1956) Analysis of elliptical bearings Trans. ASME, 78: 965.
2. Pinkus O, Mass WL (1956) Power losses in elliptical and three lobe bearings Trans. ASME, 78: 899.
3. Skinkle JM, Hornung RG (1965) Frictional characteristics of liquid hydrostatic bearings. J Basic Eng 87: 63-169.
4. Wilcock DF (1967) Externally pressurized bearings as servomechanisms. I—The Simple Thrust Bearing. J Tribol 89: 418-424.
5. Lund J (1968) Rotor-bearing dynamics design technology, Part VII: The three-lobe bearing and floating ring bearing Technical Report AFAPL-TR: 64-45.
6. Floberg L (1968) On hydrodynamic lubrication with special reference to sub-cavity pressures and number of streamers in cavitations region. Acta Poly Scand.
7. Ghigliazza R, Michelin RC (1968) Comparative investigation of friction in externally pressurized journal bearing, Wear 12: 241-256.
8. Micheli KC, Ghigliazza R (1968) Optimum geometrical design of multipad externally pressurized journal bearings. Meccanica 3: 231-241.
9. Falkenhagen GL, Gunter EJ and Shuller FT (1972) Stability and transient motion of a vertical three-lobe bearing system. Trans J Engg Ind 94: 665-677.
10. Lund W, Thomson KK (1978) A Calculation Method and Data for the Dynamic Coefficients of Oil Lubricated Journal Bearings. Proceedings of the ASME Design and Engineering Conference, Minneapolis.
11. Malik M (1983) A comparative study of some two-lobed journal bearing configurations. Tribology Transactions 26: 118-124.
12. Goenka PK, Booker JF (1983) Effect of surface ellipticity on dynamically loaded cylindrical bearing. Journal of Lubrication Technology, 105:1-12
13. Pai R, Majumdar BC (1992) Stability of submerged four-lobe oil journal bearing under dynamic load. Wear 154: 95-108.
14. Ghosh MK, Satish MR (2003) Stability of multilobe hybrid bearing with short sills—part II. Tribology International 36: 633-636.
15. Ghosh MK and Satish MR (2003) Rotor dynamic characteristics of multilobe hybrid bearings. Tribology International 36: 625-632.
16. Ghosh MK, Nagraj A (2004) Rotor dynamic characteristics of a multilobe hybrid journal bearing in turbulent lubrication. Proceedings of the Institution of Mechanical Engineers, Journal of Engineering Tribology, 218: 61-67.
17. Reynolds O (1889) On the theory of lubrication and its application to Mr. Beauchamps Tower's Experiments, including an experimental determination of the viscosity of olive oil. Phil. Trans. Roy. Soc. 177:157-234.
18. Majumdar BC (2011-2012) Introduction to Tribology of Bearings. S.Chand, New Delhi, India.
19. Hamrock BJ (1994) Fundamentals of film lubrication. McGraw-Hill: 244-252.